



VCP and PSMF1: Antagonistic regulators of proteasome activity



Christoph S. Clemen^{a,*}, Marija Marko^a, Karl-Heinz Strucksberg^a, Juliane Behrens^a, Ilka Wittig^b, Linda Gärtner^c, Lilli Winter^d, Frederic Chevessier^d, Jan Matthias^a, Matthias Türk^e, Karthikeyan Tangavelou^a, Johanna Schütz^d, Khalid Arhzaouy^a, Karsten Klopffleisch^f, Franz-Georg Hanisch^g, Wolfgang Rottbauer^c, Ingmar Blümcke^d, Steffen Just^c, Ludwig Eichinger^a, Andreas Hofmann^{h,i}, Rolf Schröder^{d,**}

^a Institute of Biochemistry I, Medical Faculty, University of Cologne, 50931 Cologne, Germany

^b Functional Proteomics, SFB815 Core Unit, Medical Faculty, Goethe University, 60590 Frankfurt, Germany

^c Molecular Cardiology, Department of Internal Medicine II, University Hospital Ulm, 89081 Ulm, Germany

^d Institute of Neuropathology, University Hospital Erlangen, 91054 Erlangen, Germany

^e Department of Neurology, University Hospital Erlangen, 91054 Erlangen, Germany

^f Institute of Genetics, University of Cologne, 50674 Cologne, Germany

^g Institute of Biochemistry II, Medical Faculty, and Center for Molecular Medicine Cologne, University of Cologne, 50931 Cologne, Germany

^h Structural Chemistry Program, Eskitis Institute, Griffith University, Queensland 4111, Australia

ⁱ Faculty of Veterinary Science, The University of Melbourne, Victoria 3030, Australia

ARTICLE INFO

Article history:

Received 1 June 2015

Accepted 12 June 2015

Available online 15 June 2015

Keywords:

Proteasome

Protein quality control

VCP

p97

Triple-A ATPase

PSMF1

Proteasome inhibitor PI31

Regulation

Mouse model

Dictyostelium discoideum

ABSTRACT

Protein turnover and quality control by the proteasome is of paramount importance for cell homeostasis. Dysfunction of the proteasome is associated with aging processes and human diseases such as neurodegeneration, cardiomyopathy, and cancer. The regulation, i.e. activation and inhibition of this fundamentally important protein degradation system, is still widely unexplored. We demonstrate here that the evolutionarily highly conserved type II triple-A ATPase VCP and the proteasome inhibitor PSMF1/PI31 interact directly, and antagonistically regulate proteasomal activity. Our data provide novel insights into the regulation of proteasomal activity.

© 2015 The Authors. Published by Elsevier Inc. This is an open access article under the CC BY-NC-ND license (<http://creativecommons.org/licenses/by-nc-nd/4.0/>).

1. Introduction

Homeostasis of cells is highly dependent on the integrity of the proteasome, which hydrolyzes intracellular proteins into small peptides, thus regulating protein turnover and removal of misfolded and poly-ubiquitinated proteins [1,2]. Proteasome dysfunction has been implicated in a wide variety of human diseases

* Corresponding author. Institute of Biochemistry I, Medical Faculty, University of Cologne, Joseph-Stelzmann-Str. 52, 50931 Cologne, Germany.

** Corresponding author. Institute of Neuropathology, University Hospital Erlangen, Schwabachanlage 6, 91054 Erlangen, Germany.

E-mail addresses: christoph.clemen@uni-koeln.de (C.S. Clemen), rolf.schroeder@uk-erlangen.de (R. Schröder).

including neurodegenerative disorders, muscular dystrophies, cardiomyopathies, immune defects, metabolic diseases, and cancer [3,4].

The 20S core of the proteasome is a 700 kDa barrel-shaped structure composed of four stacked rings. The two outer rings are formed by seven different α -subunits (PSMA1–7 in mammals) that function as entry sites, whereas the two inner rings, which consist of seven different β -subunits (PSMB1–7), exert the trypsin-, chymotrypsin-, and caspase-like proteolytic activities. Regulation of the proteasome is a complex and partially unresolved issue. Activation of the 20S core under physiological conditions requires binding of the 19S regulatory particle (synonym PA700) to one of the outer rings leading to the formation of the functionally active 26S proteasome. Alternatively, the 20S core can be activated by

other components such as the PA28 α/β hetero- and PA28 γ multimers (11S complexes), and the PA200 (PSME4) monomer [1,2,5,6]. Physiological inhibition of the proteasome is achieved by PSMF1 (proteasome inhibitor PI31 subunit [7]) binding. PSMF1 is a highly conserved, proline-rich 31 kDa protein that inhibits the proteasomal activities by either direct binding to the outer rings of the 20S proteasome or by competing with the activating particles for 20S binding [8–10].

VCP (valosin containing protein; orthologs known as VAT, CDC48, CdcD, TER94, p97) is a ubiquitously expressed and evolutionarily highly conserved type II triple-A ATPase involved in a wide variety of essential cellular processes comprising nuclear envelope reconstruction, the cell cycle, post-mitotic Golgi reassembly, suppression of apoptosis, DNA damage response, and protein quality control mechanisms [11]. The essential role of VCP in human cells is highlighted by the observation that point mutations of the VCP gene cause three autosomal dominant disorders, namely IBM/IFD (inclusion body myopathy with early onset Paget's disease of bone and frontotemporal dementia) [12], ALS14 (amyotrophic lateral sclerosis with or without frontotemporal dementia) [13], and a form of HSP (hereditary spastic paraplegia) [14].

Here, we demonstrate that VCP and PSMF1 interact directly, and regulate the activity of the fundamentally important proteasome in an antagonistic fashion.

2. Materials and methods

2.1. Lumier technique

The luminescence-based mammalian interactome mapping (Lumier) technique allows detection and quantitation of protein–protein interactions in mammalian cells [15]. The method is based on a double-transfection with plasmids coding for the proteins of interest with either a Renilla luciferase or a Protein A tag. The original protocol of the Lumier technique was modified, optimized, and used as described in the [Supplementary Materials and Methods section](#).

2.2. Proteasomal activity assays

In this study, the chymotrypsin-like proteasomal activity was monitored based on the cleavage of succinyl-LLVY-aminoluciferin. In a secondary reaction, the released aminoluciferin is processed by the Firefly luciferase and used for luminometry. This luminescence-based technique has the experimental advantage that it allows a direct determination of the proteasomal activity during the entire course of the experiment. In contrast, the commonly used fluorescence-based assay detects the increment of the 7-amino-4-methylcoumarin cleavage product thus limiting the measurement to the initial state. For details on our optimized protocol please refer to the [Supplementary Materials and Methods Section](#).

2.3. Molecular modeling

N-PSMF1 (PDB entry 2VT8), VCP-ND1 (PDB entry 3QQ8), FAFA1-UBX in complex with the VCP-ND1 domain (PDB entry 3QQ8), and 20S proteasome (PDB entry 1YAU) were used for rigid body docking. Initial complexes of N-PSMF1:VCP-ND1 and [N-PSMF1]₇:20S were then subjected to molecular dynamics simulations ($t = 22.5$ ns and $t = 10$ ns, respectively). Detailed information on the molecular modeling procedures is provided in the [Supplementary Materials and Methods Section](#).

2.4. Miscellaneous methods

Further standard methods and an antibody list are given in the [Supplementary Materials and Methods Section](#). Generation of mice haploinsufficient for VCP is described in the legend to [Fig. S1](#).

3. Results

3.1. VCP directly interacts with the proteasome inhibitor PSMF1

To identify novel and disease relevant VCP binding partners, we have previously performed VCP co-immunoprecipitation experiments, which resulted in the identification of PSMF1 as a putative candidate (Supplementary Tables 1 and 2 in Ref. [16]). By means of luminescence-based mammalian interactome mapping (Lumier) [15], we investigated potential interactions of VCP with various target proteins. Using this novel experimental approach, we first confirmed VCP multimer formation ([Fig. 1A](#)) as well as its interactions with the previously established VCP binding partners Ufd1 and Npl4. More importantly, we could demonstrate an interaction of VCP and PSMF1 within a similar dynamic range as observed for VCP and Ufd1 or Npl4 ([Fig. 1B](#)). Using pull-down assays with purified recombinant proteins, we could validate that VCP and its novel binding partner PSMF1 interact directly ([Fig. 1C](#)).

3.2. Reduced VCP levels cause decreased proteasomal activity

Previous studies showed that the targeted ablation of VCP in mouse, fruit fly, yeast, and the protist *Trypanosoma brucei* was lethal in all these organisms [17–20]. In VCP haploinsufficient mice ([Fig. S1](#)), which displayed a ~30% and ~40% reduction of the VCP mRNA and protein levels, respectively ([Fig. 2A–C](#)), we noted an increase of poly-ubiquitinated proteins ([Fig. 2C](#)). Using a highly sensitive luminescence-based proteasomal activity assay, we studied the chymotrypsin-like activity in lower hind limb muscles derived from three months old mice. Here, the VCP haploinsufficient mice showed a significant reduction (~32%) of the specific proteasomal activity as compared to wild-type littermates ([Fig. 2D](#)), while the expression levels of 19S and 20S proteasome complexes as well as PSMF1 remained unchanged ([Fig. 2C](#)).

3.3. VCP and PSMF1 antagonistically regulate proteasome activity

To investigate potential roles of VCP and PSMF1 on proteasomal activity *in vitro*, we first added purified recombinant human VCP (100% sequence identity to murine VCP) to skeletal muscle lysates derived from the VCP haploinsufficient mice. This resulted in a dose-dependent increase of proteasomal activity ([Fig. 3A](#)). This effect, however, was not observed in analogous experiments using either purified human 26S or 20S proteasomes instead of the tissue lysate ([Fig. 3B](#)). The latter finding argues against a direct stimulatory effect of VCP on the proteasome and favors the presence of a co-factor in the tissue lysate.

We considered PSMF1 as a promising candidate and therefore used both purified recombinant VCP and PSMF1 proteins to analyze their activating and inhibiting effects on 20S proteasomal activity *in vitro* ([Fig. 3C](#)). Upon addition of VCP, the activity of purified proteasome remained unchanged ([Fig. 3C](#), part i, red line), whereas the addition of PSMF1 inhibited proteasomal activity as expected (part i, blue line). The subsequent addition of PSMF1 to the reaction already containing VCP significantly reduced proteasomal activity (part ii, red line). The addition of VCP to the reactions containing PSMF1 antagonized the inhibitory effects (part iii, red and blue lines) and resulted in a significant increase in proteasomal activity. The subsequent addition of more PSMF1 resulted again in

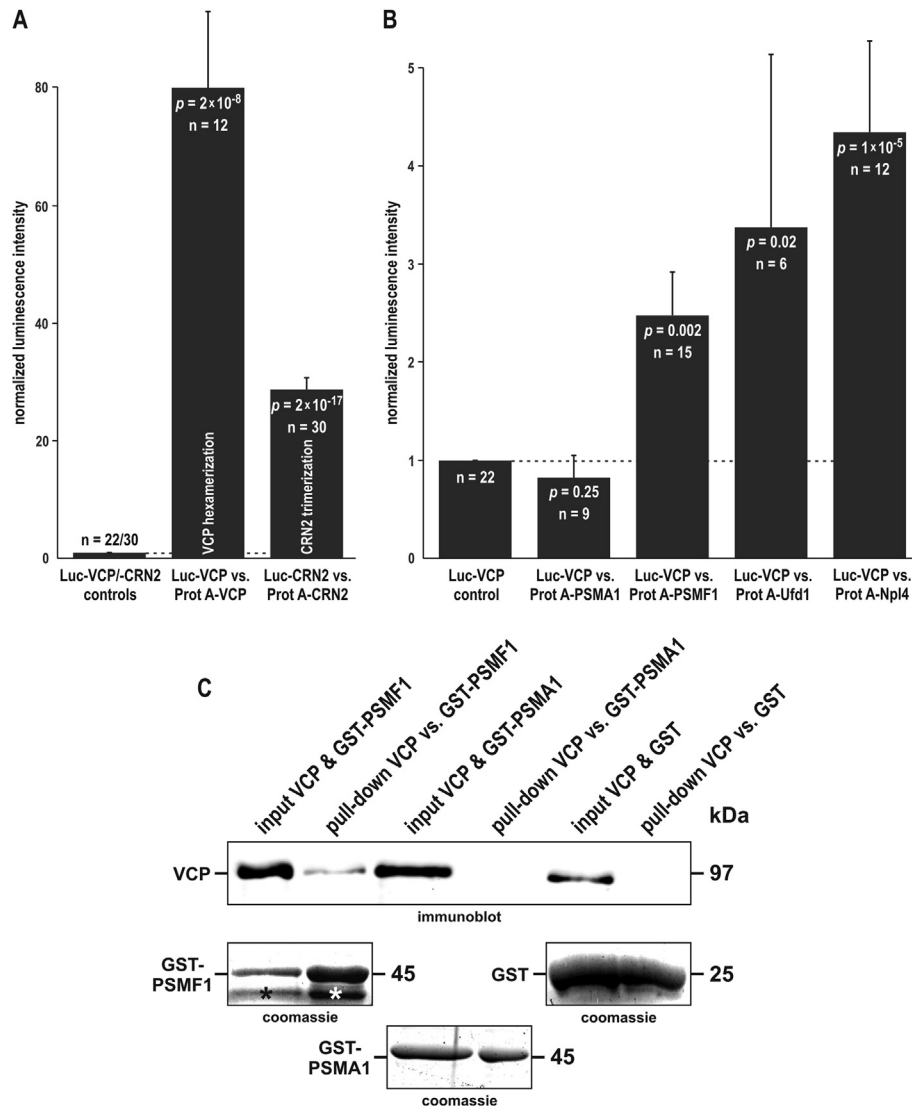


Fig. 1. VCP interacts directly with PSMF1 (proteasome inhibitor PI31 subunit). A, B, VCP protein interaction analyses using the Lumier-technique, which is based on a double-transfection with plasmids coding for Renilla luciferase- (Luc) and Protein A- (Prot A) tagged proteins. Negative controls (normalized luminescence signal intensity set to 1, dotted lines, left columns in A and B) are based on the sole transfection of the luciferase-tagged proteins. Statistical significance was calculated by Student's t-test; n indicates the number of independent experiments; error bars indicate standard errors of the mean. A, the high normalized luminescence signal intensity of VCP reflects its hexamerization state. To visualize the dynamic range of the Lumier method, the luminescence of a coronin protein (CRN2/Coro1C) that forms trimers is shown. B, lumier analysis shows binding of VCP to PSMF1 with binding strength similar to those of the two well-established VCP binding partners Ufd1 and Npl4. Further, the Lumier method showed a lack of interaction of VCP with the 20S proteasome subunit PSMA1. C, confirmation of the direct VCP – PSMF1 interaction by pull-down assays employing purified recombinant human VCP (untagged) and PSMF1 (GST-tagged) proteins. Negative controls were GST-PSMA1 and GST alone. Asterisks, degradation products of PSMF1 as determined by mass spectrometry. For illustration, the original immunoblots were cropped to display the relevant sections.

inhibition of proteasomal activity (part iv), which, in turn, could be reversed by further addition of VCP (data not shown). To assess the molar ratios of the reaction mixtures, proteins were precipitated at the end of the experiments. Analysis by SDS-PAGE showed that the observed effects of PSMF1 and VCP on the proteasomal activity are stoichiometric (Fig. 3D; ratios are indicated).

We previously reported that a strain of the model organism *Dictyostelium discoideum* deficient for the core autophagy protein ATG9 (ATG9^{KO} strain) has an intrinsic and severe defect of proteasomal activity [21]. To assess whether VCP can also influence the proteasomal activity *in vivo*, we utilized this strain and over-expressed RFP-tagged VCP in the ATG9^{KO} cells. Here, we found that an approximately 2-fold increase of VCP protein levels (data not shown) fully restored the proteasomal activity (Fig. 3E).

3.4. PSMF1 may act as a multimer

It is currently unknown whether the PSMF1-induced inactivation of the proteasome is due to binding of monomeric or multimeric PSMF1 to the 20S core. Therefore, we performed *in silico* analyses, which indicated that multimers of PSMF1 may bind in place of 19S regulatory particles and thus lead to the formation of catalytically inactive [PSMF1]_n:20S proteasome complexes. The simulated model shown here assumes n = 7, i.e. a heptameric ring of PSMF1 on top of the 20S proteasome (Fig. 4A); however, we cannot exclude the possibility of a hexameric PSMF1 assembly on the 20S particle. Experimental evidence for PSMF1 multimers comes from clear-native PAGE analyses, which indicated the formation of trimers, hexamers, and nonamers (Fig. 4B).

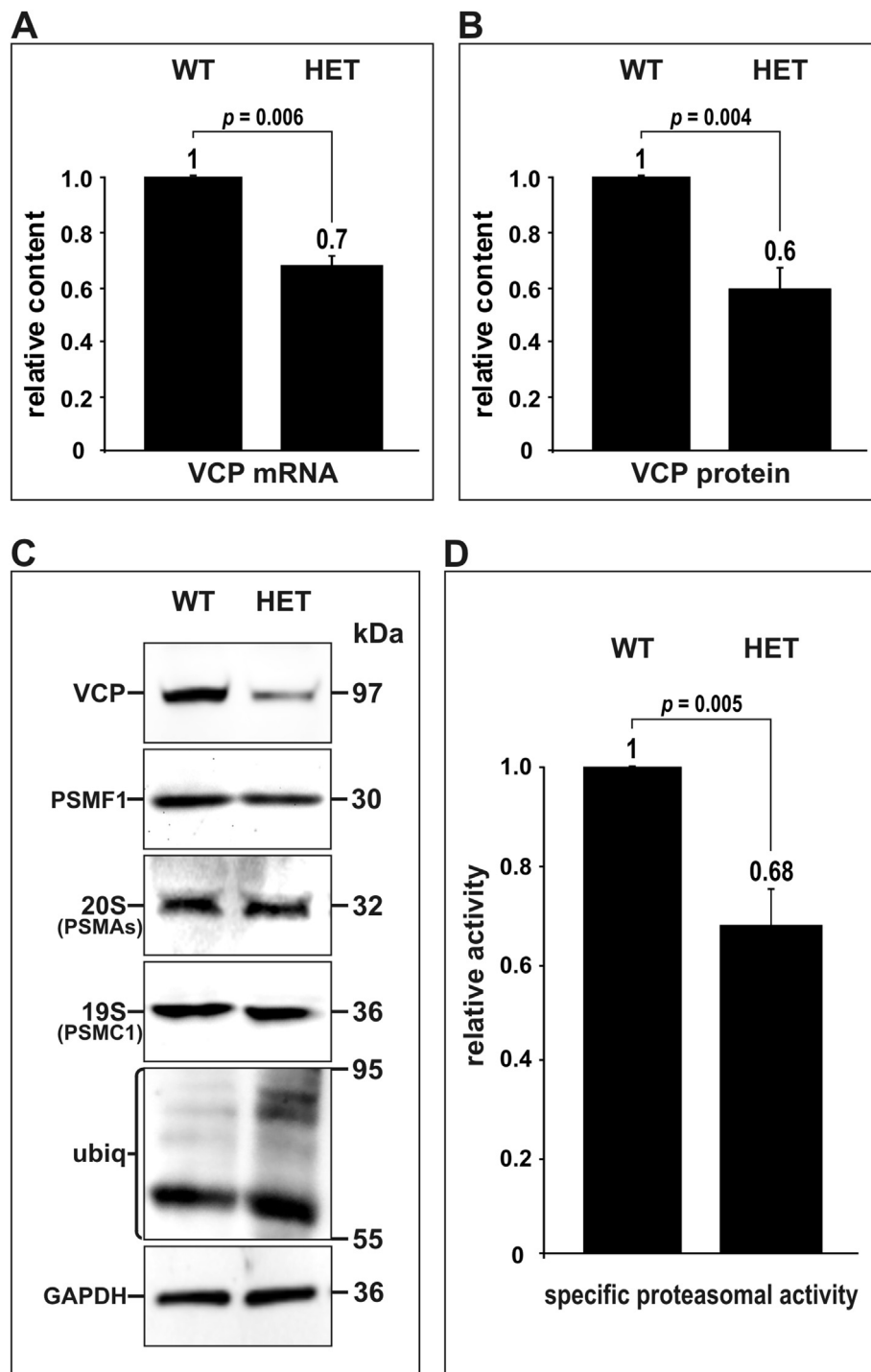


Fig. 2. VCP haploinsufficient mice show reduced specific proteasomal activity and increased protein ubiquitination. A, quantitative real-time RT-PCR analyses of VCP mRNA expression in skeletal muscle tissue derived from wild-type (WT) and heterozygous (HET) congenic B6J.129S2-*Vcp*^{tm1(ko)CscI&Rftr} mice. Mean values and standard errors were obtained by four-fold repeated measurements in two animals per genotype. B, densitometric analyses of VCP immunoblots. Mean values and standard errors were calculated by analyzing 25 and 29 bands derived from wild-type and heterozygous mice, respectively. Columns in A and B represent relative values with wild-type expression scaled to 1. *p*-values were calculated by Student's *t*-test. The reduced levels of VCP mRNA and protein demonstrate a VCP haploinsufficiency. C, the reduced VCP protein expression level is associated with increased protein ubiquitination (ubiq; note that this is a pattern of increased ubiquitination levels typical for skeletal muscle), whereas the levels of PSMF1, 19S, and 20S proteasome were unchanged. GAPDH was used as loading control. For illustration, the original immunoblots were cropped to display the relevant sections. D, luminescence-based proteasomal activity measurements in skeletal muscle tissue from lower hind limbs of three months old mice. The specific proteasomal activity is normalized to the amount of proteasome. Note that the chymotrypsin-like proteasomal activity in VCP haploinsufficient mice is significantly reduced. Mean values and standard errors were obtained from six independent experiments; *p*-values were calculated by Student's *t*-test; activity of wild-type mice was set to 1.

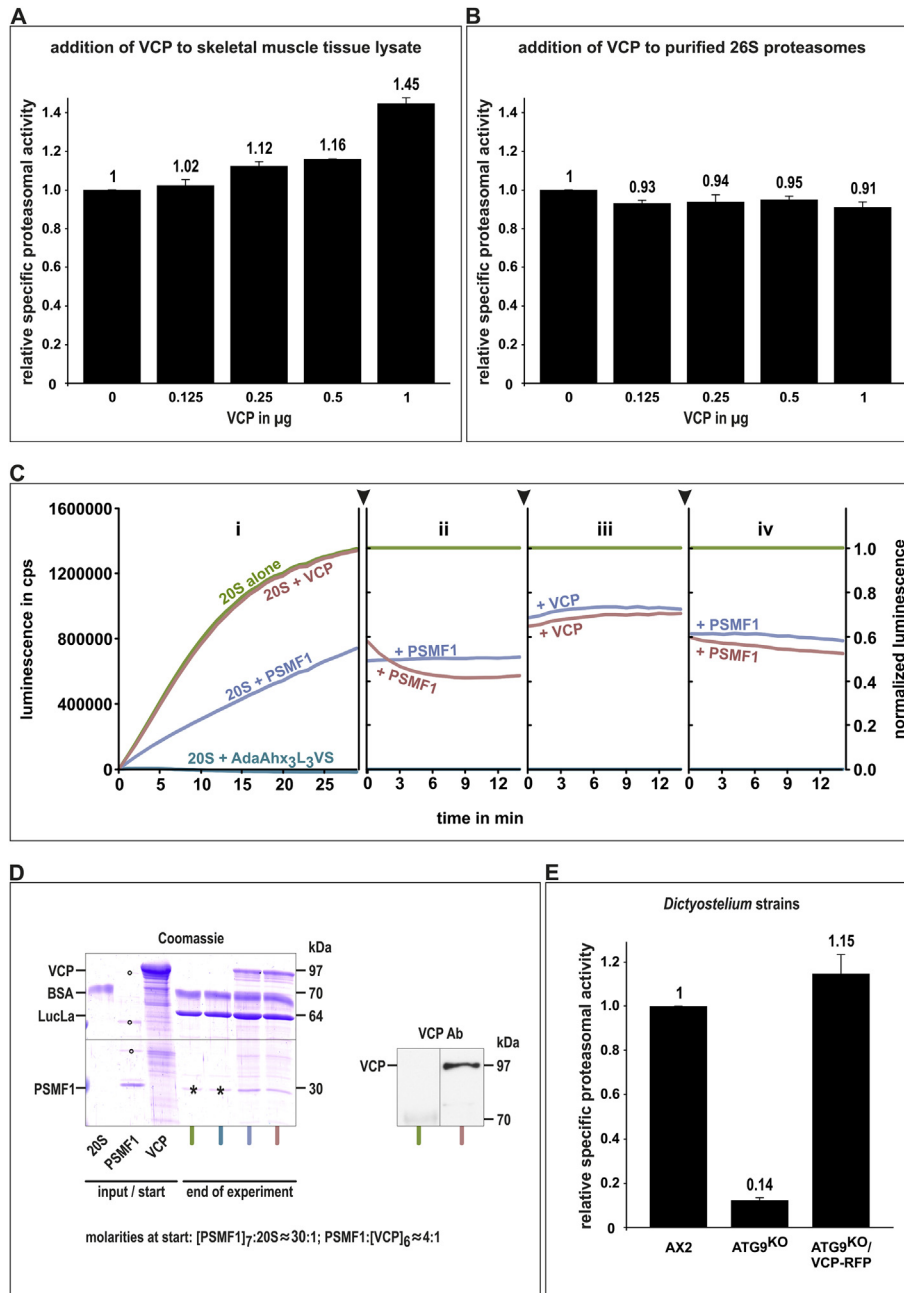


Fig. 3. VCP and PSMF1: antagonistic regulators of proteasomal activity. **A**, addition of recombinant human VCP to lysates prepared from skeletal muscle tissue derived from VCP haploinsufficient mice increased proteasomal activity in a dose dependent manner. Mean values and standard errors were obtained from two independent experiments. Columns represent relative values of the normalized chymotrypsin-like activity; proteasomal activity without addition of VCP was set to 1. **B**, in a corresponding assay using a purchased preparation of human 26S proteasome derived from HEK293 cells, VCP did not increase proteasomal activity. **C**, luminescence-based proteasomal activity of human 20S proteasome derived from red blood cells alone, or in the presence of either proteasomal inhibitor AdaAhx₃L₃VS, or recombinant human VCP purified from bacteria, or recombinant human PSMF1 purified from HEK293 cells. Reactions were monitored until steady-state was reached (panel (i); y-axis: counts per second). The reactions were continued after the addition of PSMF1 or VCP as indicated by the arrowheads (panels (ii)–(iv); y-axis: normalized activity; activity of 20S alone was used as reference and set to 1). Gaps before the arrowheads indicate a delay of three minutes before measurements were resumed after each protein addition. The data shown were derived from a single continuous experiment that had been independently conducted three times with the same experimental design; three more experiments with identical results employed 20S proteasome prepared from 293T cells in conjunction with recombinant human GST-PSMF1 purified from *E. coli*. **D**, visualization of the stoichiometry of PSMF1 and VCP used in **C**. Proteins of the reaction mixtures in **C** (see the color codes) were chloroform-methanol precipitated after completion of the reactions, separated by SDS-PAGE, and stained by Coomassie brilliant blue (the horizontal line within the image indicates different contrast adjustments made to the upper and lower parts). Since only 100 ng of proteasome were used per reaction, subunits of the proteasome are not visible; the single band at approximately 70 kDa corresponds to BSA present in the proteasome buffer. Contaminations of purified PSMF1 with bovine actin and tubulin as well as horse Hsp90 are indicated by open circles. Reactions annotated with an asterisk did not receive PSMF1, but contained a BSA fragment of similar size as determined by mass spectrometry. The prominent band at 64 kDa corresponds to the recombinant Firefly luciferase (LucLa). Molar ratios of PSMF1 to 20S proteasome and of PSMF1 to VCP at the start of the experiment are indicated. VCP immunoblotting confirmed that the proteasome preparations were free of VCP that may have been co-purified (the two lines shown were digitally rearranged to omit dispensable lines). **E**, *in vivo* rescue of the specific proteasomal activity by over-expression of RFP-tagged VCP in a previously reported *D. discoideum* ATG9^{KO} strain, which exhibits a drastically reduced proteasomal activity [21]. Activity of AX2 wild-type cells was set to 1. We previously reported a similar finding [21], however, for the purpose of the present study we had performed three additional measurements to further substantiate the initial finding.

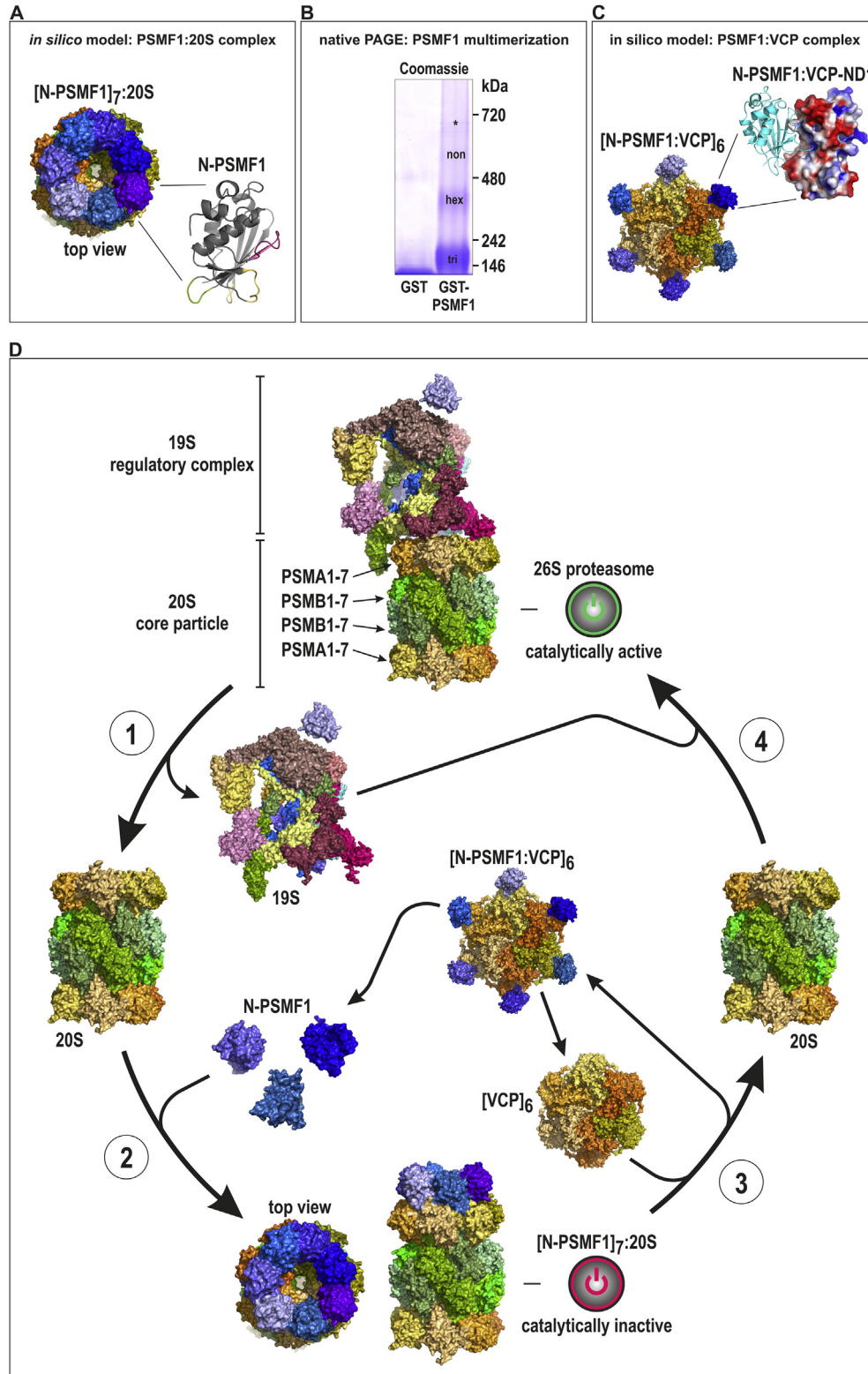


Fig. 4. PSMF1 interactions with 20S proteasome and VCP: a model for the antagonistic regulation of proteasomal activity. **A**, *in silico* model of a PSMF1 multimer replacing the 19S regulatory particle leading to the formation of a catalytically inactive [N-PSMF1]_n:20S proteasome (for illustration, n = 7). The N-terminal ends of N-PSMF1 project radially to the outside and the C-terminal ends into the inner cavity of the heptameric ring. The putative binding site of an N-PSMF1 monomer (cartoon representation of secondary structure elements) to the PSMA1-7 ring is indicated in green, the binding site to VCP in magenta; the latter contains the amino acid sequence LYV which matches an HbYX motif that is well-known for modulators of proteasomal activity. The amino acid stretch given in yellow represents putative interaction interfaces with both the proteasome and VCP. **B**, recombinant purified GST-PSMF1 and GST were separated by clear-native PAGE. Whereas GST remains monomeric, PSMF1 forms trimers, hexamers, and nonamers. Asterisk, contamination by bacterial GroEL, as determined by mass spectrometry. **C**, *in silico* model of the PSMF1-VCP interaction. N-PSMF1:VCP-ND1 illustrates the potential binding mode of N-PSMF1 (cartoon representation in turquoise) with VCP-ND1 (surface representation with mapped electrostatics in red (negative potential) and blue (positive potential)). The equilibrated model of N-PSMF1:VCP-ND1 and the hexameric VCP structure were used to construct the [N-PSMF1:VCP]₆ complex (surface representation with PSMF1 in bluish colors and the VCP monomers in orange and green). **D**, model of the PSMF1 and VCP mediated antagonistic regulation of proteasomal activity. Surface representations of the 26S proteasome (electron microscopy reconstruction, PDB entry 4C0V), N-PSMF1 and VCP. See Discussion section for details.

The binding sites between PSMF1 and VCP have not yet been experimentally established. Based on the structural similarities between PSMF1 and FAFA1-UBX, another VCP binding partner, we performed molecular modeling addressing the PSMF1-VCP interaction. As a result of our *in silico* modeling, the complex of N-PSMF1:VCP-ND1 (Fig. 4C) illustrates the putative binding mode of N-PSMF1 (cartoon representation in turquoise) with VCP-ND1 (surface representation with mapped electrostatics in red (negative potential) and blue (positive potential)). VCP assembles into hexamers with its ATPase domains forming a central cylinder that is surrounded by the N-terminal CDC48 domains [22]. We therefore used the N-PSMF1:VCP-ND1 model and the hexameric VCP structure to finally construct a [N-PSMF1:VCP]₆ complex (surface representation with PSMF1 in bluish colors and the VCP monomers in orange and green) (Fig. 4C).

4. Discussion

Beyond a multitude of other functions, VCP has also been attributed an important role in the degradation of poly-ubiquitinated proteins via the proteasome. A knock-down of VCP in HeLa cells led to the accumulation of poly-ubiquitinated proteins [23]. Previous studies demonstrated that several substrates of the ubiquitin-proteasomal system need VCP and its co-factors in order to be properly processed [24,25]. Moreover, VCP was detected in proteasomal purifications [26–29], and a more recent study demonstrated that VCP associated with the 19S sub-complex of the proteasome upon proteasomal inhibition or over-expression of VCP. This study also indicated that the VCP co-factors Ufd1 and Npl4 promote an enrichment of VCP at the inhibited proteasome [30].

PSMF1 on the other hand was generally described as a potent inhibitor of proteasomal activity [7–10]. In contrast, a recent study suggested that the situation may be more complex as ADP-ribosylated PSMF1 may stimulate proteasomal activity [8]. This latter mechanism relies on abolished binding of the post-translationally modified PSMF1 to the 20S proteasome core, which instead binds and sequesters 19S assembly chaperones, thus liberating 19S regulatory particles for the formation of catalytically active 26S proteasomes. However, this suggestion has been challenged by the findings that the ribosylation inhibitor XAV939 did not decrease proteasomal activity, and that ADP-ribosylation of PSMF1 could not be detected by immunoblotting [31].

Based on our experimental work in conjunction with *in silico* modeling, we delineate an extended mechanism of proteasome regulation, in which PSMF1 and VCP antagonistically regulate proteasomal activity (Fig. 4D). The catalytically active 26S proteasome (top) continually assembles and disassembles *in vivo* into the 20S core particle and the 19S regulatory complex (transition 1). Only the “free” 20S proteasome (left) seems to interact with PSMF1 (transition 2), as a recent study showed that PSMF1 was able to suppress the assembly of 26S proteasome from 19S and 20S particles, but had no effect on preformed 26S proteasome *in vitro* [31]. The catalytically inactive state of the proteasome is the [PSMF1]_n:20S complex (bottom; PSMF1 in bluish colors, for illustration, n = 7). As previously proposed [10], PSMF1 molecules may indeed act as caps of the 20S proteasomes with the C-terminal regions of the PSMF1 monomers blocking the entry of substrates to the proteolytically active sites inside the 20S core particle. This PSMF1-mediated inactivation of the proteasome can be counteracted by increasing levels of VCP. In our mechanistic model, VCP sequesters PSMF1 from the [PSMF1]_n:20S complex and gives rise to [PSMF1:VCP]₆ complexes (transition 3). This finally enables the re-assembly of catalytically active 26S proteasomes from “free” 20S core and 19S regulatory particles (transition 4).

We thus propose that in addition to its postulated roles of extracting misfolded proteins from the ER and shuttling poly-ubiquitinated proteins to the proteasome [32,33], VCP activates the proteasome by counteracting the inhibitory effect of PSMF1. Importantly, our model does not exclude activation of the proteasome by ADP-ribosylation of PSMF1 [8]. Both regulatory mechanisms would lead to re-assembly and activation of the 26S proteasome and facilitate the turnover of degradation-prone proteins. Our data thus provide novel, fundamental insights into the basic regulation of proteasomal activity.

Acknowledgments

We thank Carolin Berwanger and Maria Stumpf for excellent technical assistance. Ufd1 and Npl4 expression plasmids were kindly provided by Annett Bödrich (Max Delbrück Center for Molecular Medicine, Berlin, Germany) and Hemmo Meyer (University of Duisburg-Essen, Germany), respectively. pDEST-RLuc (originally named pcDNA3-RLuc-GW) and pDEST-ProtA (originally named pTREN-Dest30-ProtA) vectors for the Lumier experiments were generously provided by Manfred Kögl (Preclinical Target Development, and Genomics and Proteomics Core Facilities, DKFZ, Heidelberg, Germany).

Grant support by the German Research Foundation (DFG) within the framework of the multi-location research group FOR1228 (grants CL 381/3-2 to CSC, HA 2092/23-2 to FGH, RO 2173/4-2 to WR, JU 2859/1-2 to SJ, EI 399/7-2 to LE, and SCHR 562/9-2 to RS), within the collaborative research consortium 815 (project Z1 to IW), and for individual research projects (grants CL 381/1-1 to CSC and SCHR 562/7-1 to RS), by the Fritz-Thyssen-Foundation (grant 10.071.165 to RS and CSC), the Australian Research Council (ARC) (grant LE120100071 to AH), by Köln Fortune (to CSC and LE), and by the Interdisciplinary Center for Clinical Research (IZKF) of the Clinical Center Erlangen (to MT) is gratefully acknowledged.

Appendix A. Supplementary data

Supplementary data related to this article can be found at <http://dx.doi.org/10.1016/j.bbrc.2015.06.086>.

Transparency document

Transparency document related to this article can be found online at <http://dx.doi.org/10.1016/j.bbrc.2015.06.086>.

References

- [1] A.V. Sorokin, E.R. Kim, L.P. Ovchinnikov, Proteasome system of protein degradation and processing, *Biochemistry (Mosc)* 74 (2009) 1411–1442.
- [2] T. Jung, B. Catalgol, T. Grune, The proteasomal system, *Mol. Asp. Med.* 30 (2009) 191–296.
- [3] A.V. Gomes, Genetics of proteasome diseases, *Scientifica* 2013 (2013) 629–637.
- [4] E. Jankowska, J. Stoj, P. Karpowicz, et al., The proteasome in health and disease, *Curr. Pharm. Des.* 19 (2013) 1010–1028.
- [5] M. Rechsteiner, C.P. Hill, Mobilizing the proteolytic machine: cell biological roles of proteasome activators and inhibitors, *Trends Cell Biol.* 15 (2005) 27–33.
- [6] B. Dahlmann, Proteasomes, *Essays Biochem.* 41 (2005) 31–48.
- [7] M. Chu-Ping, C.A. Slaughter, G.N. DeMartino, Purification and characterization of a protein inhibitor of the 20S proteasome (macropain), *Biochim. Biophys. Acta* 1119 (1992) 303–311.
- [8] P.F. Cho-Park, H. Steller, Proteasome regulation by ADP-ribosylation, *Cell* 153 (2013) 614–627.
- [9] D.M. Zais, S. Standera, H. Holzhtutter, et al., The proteasome inhibitor PI31 competes with PA28 for binding to 20S proteasomes, *FEBS Lett.* 457 (1999) 333–338.
- [10] S.L. McCutchen-Maloney, K. Matsuda, N. Shimbara, et al., cDNA cloning, expression, and functional characterization of PI31, a proline-rich inhibitor of the proteasome, *J. Biol. Chem.* 275 (2000) 18557–18565.

- [11] G.H. Baek, H. Cheng, V. Choe, et al., Cdc48: a Swiss army knife of cell biology, *J. Amino Acids* 2013 (2013), 183421.
- [12] G.D. Watts, J. Wymer, M.J. Kovach, et al., Inclusion body myopathy associated with Paget disease of bone and frontotemporal dementia is caused by mutant valosin-containing protein, *Nat. Genet.* 36 (2004) 377–381.
- [13] J.O. Johnson, J. Mandrioli, M. Benatar, et al., Exome sequencing reveals VCP mutations as a cause of familial ALS, *Neuron* 68 (2010) 857–864.
- [14] S.T. de Bot, H.J. Schelhaas, E.J. Kamsteeg, et al., Hereditary spastic paraplegia caused by a mutation in the VCP gene, *Brain* 135 (2012) e223.
- [15] M. Barrios-Rodiles, K.R. Brown, B. Ozdamar, et al., High-throughput mapping of a dynamic signaling network in mammalian cells, *Science* 307 (2005) 1621–1625.
- [16] C.S. Clemen, K. Tangavelou, K.H. Strucksberg, et al., Strumpellin is a novel valosin-containing protein binding partner linking hereditary spastic paraplegia to protein aggregation diseases, *Brain* 133 (2010) 2920–2941.
- [17] J.M. Müller, K. Deinhardt, I. Rosewell, et al., Targeted deletion of p97 (VCP/CDC48) in mouse results in early embryonic lethality, *Biochem. Biophys. Res. Commun.* 354 (2007) 459–465.
- [18] K.U. Fröhlich, H.W. Fries, M. Rudiger, et al., Yeast cell cycle protein CDC48p shows full-length homology to the mammalian protein VCP and is a member of a protein family involved in secretion, peroxisome formation, and gene expression, *J. Cell Biol.* 114 (1991) 443–453.
- [19] J.R. Lamb, V. Fu, E. Wirtz, et al., Functional analysis of the trypanosomal AAA protein TbVCP with trans-dominant ATP hydrolysis mutants, *J. Biol. Chem.* 276 (2001) 21512–21520.
- [20] A. Leon, D. McKearin, Identification of TER94, an AAA ATPase protein, as a bam-dependent component of the *Drosophila* fusome, *Mol. Biol. Cell* 10 (1999) 3825–3834.
- [21] K. Arhzaouy, K.H. Strucksberg, S.M. Tung, et al., Heteromeric p97/p97(R155C) complexes induce dominant negative changes in wild-type and autophagy 9-deficient dictyostelium strains, *PloS One* 7 (2012) e46879.
- [22] B. DeLaBarre, A.T. Brunger, Complete structure of p97/valosin-containing protein reveals communication between nucleotide domains, *Nat. Struct. Biol.* 10 (2003) 856–863.
- [23] C. Wojcik, M. Yano, G.N. DeMartino, RNA interference of valosin-containing protein (VCP/p97) reveals multiple cellular roles linked to ubiquitin/proteasome-dependent proteolysis, *J. Cell Sci.* 117 (2004) 281–292.
- [24] F. Förster, J.M. Schuller, P. Unverdorben, et al., Emerging mechanistic insights into AAA complexes regulating proteasomal degradation, *Biomolecules* 4 (2014) 774–794.
- [25] T. Zhang, Y. Ye, The final moments of misfolded proteins en route to the proteasome, *DNA Cell Biol.* 33 (2014) 477–483.
- [26] H.C. Besche, W. Haas, S.P. Gygi, et al., Isolation of mammalian 26S proteasomes and p97/VCP complexes using the ubiquitin-like domain from HHR23B reveals novel proteasome-associated proteins, *Biochemistry* 48 (2009) 2538–2549.
- [27] C. Guerrero, T. Milenkovic, N. Przulj, et al., Characterization of the proteasome interaction network using a QTAX-based tag-team strategy and protein interaction network analysis, *Proc. Natl. Acad. Sci. U. S. A.* 105 (2008) 13333–13338.
- [28] T. Shibatani, E.J. Carlson, F. Larabee, et al., Global organization and function of mammalian cytosolic proteasome pools: implications for PA28 and 19S regulatory complexes, *Mol. Biol. Cell* 17 (2006) 4962–4971.
- [29] R.M. Dai, E. Chen, D.L. Longo, et al., Involvement of valosin-containing protein, an ATPase co-purified with IkappaBalpha and 26 S proteasome, in ubiquitin-proteasome-mediated degradation of IkappaBalpha, *J. Biol. Chem.* 273 (1998) 3562–3573.
- [30] E. Isakov, A. Stanhill, Stalled proteasomes are directly relieved by P97 recruitment, *J. Biol. Chem.* 286 (2011) 30274–30283.
- [31] X. Li, D. Thompson, B. Kumar, et al., Molecular and cellular roles of PI31 (PSMF1) protein in regulation of proteasome function, *J. Biol. Chem.* 289 (2014) 17392–17405.
- [32] S. Braun, K. Matuschewski, M. Rape, et al., Role of the ubiquitin-selective CDC48(UFD1/NPL4) chaperone (segregase) in ERAD of OLE1 and other substrates, *EMBO J.* 21 (2002) 615–621.
- [33] S. Raasi, D.H. Wolf, Ubiquitin receptors and ERAD: a network of pathways to the proteasome, *Semin. Cell Dev. Biol.* 18 (2007) 780–791.